


## Article

# Design and Parameter Optimization of a Finger Clip Plate Garlic Seed-Metering Device Based on EDEM

Haoyi Wang <sup>1</sup>, Xinping Sun <sup>2</sup> , Hua Li <sup>1,\*</sup>, Jieyi Fu <sup>1</sup>, Xiaoping Zeng <sup>3</sup>, Youzhi Xu <sup>1</sup>, Yongjian Wang <sup>1</sup>, Huaqing Liu <sup>1</sup> and Zhimin Lü <sup>1</sup>

<sup>1</sup> College of Engineering, Nanjing Agricultural University, Nanjing 210031, China; 30219119@njau.edu.cn (H.W.); 9183012006@njau.edu.cn (J.F.); 9193011023@njau.edu.cn (Y.X.); yjwang@njau.edu.cn (Y.W.); 302191113@njau.edu.cn (H.L.); 302191115@njau.edu.cn (Z.L.)

<sup>2</sup> College of Mechanical and Power Engineering, Nanjing Tech University, Nanjing 211816, China; xinpingsun@njtech.edu.cn

<sup>3</sup> Jiangsu Provincial Agricultural Technology Extension Station, Nanjing 210036, China; jsnjzengxp@163.com

\* Correspondence: lihua@njau.edu.cn

**Abstract:** In present-day mechanized *garlic* seeding, high missing rates and low qualified percentages of single seeds are common problems; thus, a finger clip plate *garlic* seed-metering device was designed in this study. First, the structure and working principle of the seed-metering device were studied. Subsequently, the critical component parameters of the seed-metering device were determined using theoretical calculations; then, EDEM software was used in single-factor simulation experiments to analyze the effects of opening the diameter of the seed-collecting spoon, the operating speed of the seeding tray, and the population number on the seed-filling performance. Finally, a Box-Behnken center combination experiment was conducted with the population, opening the diameter of the seed-collecting spoon, and rotating the speed of the seeding tray as experiment factors, with the single-seed filling rate, qualified percent, and missing rate as evaluation indicators. A three-factor and three-level orthogonal test was conducted to establish the mathematic regression model of the experiment factors and evaluation indicators, as well as to realize the parameter optimization. After rounding, the laboratory validation test was carried out with 240~280 seeds, a 26 mm seed scoop-opening diameter, and a 28 r/min operating speed. The average qualified rate, missing rate, and reply rate of single seeds were 91.86%, 2.71%, and 5.43%, respectively, which is basically consistent with the forecast results of regression model.

**Keywords:** pickup finger precision seed-metering device; EDEM; *garlic*; seeding performance



**Citation:** Wang, H.; Sun, X.; Li, H.; Fu, J.; Zeng, X.; Xu, Y.; Wang, Y.; Liu, H.; Lü, Z. Design and Parameter Optimization of a Finger Clip Plate Garlic Seed-Metering Device Based on EDEM. *Agronomy* **2022**, *12*, 1543. <https://doi.org/10.3390/agronomy12071543>

Academic Editor: Simon Pearson

Received: 23 May 2022

Accepted: 23 June 2022

Published: 28 June 2022

**Publisher's Note:** MDPI stays neutral with regard to jurisdictional claims in published maps and institutional affiliations.



**Copyright:** © 2022 by the authors. Licensee MDPI, Basel, Switzerland. This article is an open access article distributed under the terms and conditions of the Creative Commons Attribution (CC BY) license (<https://creativecommons.org/licenses/by/4.0/>).

## 1. Introduction

*Garlic*, scientifically known as *allium sativum*, is an important seasoning and horticultural plant, used as a spice in food and also used as a medicine due to its many human health and wellbeing benefits [1–3].

As an industrial crop in China, *garlic* usually ranks at the top in terms of planting area, due to its high output and export volume all over the world, which greatly enhances local economic growth and farmers' income [4]. The large-scale development of *garlic* planting has promoted the transformation from manual sowing to mechanical sowing, effectively saving on labor force and improving production efficiency. Nevertheless, current research on the mechanical sowing of *garlic* is still far from advanced, and the existing seed-metering devices have a backward mechanization in the working process, so problems associated with a high reply rate and missing rate are common [5]. The accuracy of single-seed seed-metering devices is an important indicator of the performance of *garlic* seed-metering devices, which can effectively address the existing problem and improve the mechanization effect of *garlic* seeding [6]. The current *garlic* seeding modes mainly include mechanical and air suction, among which the mechanical type is the most commonly applied. This

involves the cell feed wheel, spoon belt, spoon chain, clamping-type, rotary spoon, and vibrating-type seeders. Most European and American countries prefer spoon chain seed-metering devices [7], while China typically uses rotary spoon, vibrating-type, and spoon belt seeders [8].

On the basis of the traditional seed-metering method, scholars have carried out a series of studies on the bottleneck problem of improving the qualified rate of single seeds, and reducing the replay rate and missing rate. They have designed seed-metering devices of different forms, which effectively promote the development of precise *garlic* selection and sending. Hou et al. [9] adopted the design concept of “select one from many” to develop a claw-type, circulating, single-seed, seed-metering device, with a single-seed rate of 92.52%, but this has a high missing rate, and may cause seed damage in the seed-cleaning process and blockage when grasping. Hou et al. [10] designed a double-filled *garlic* single-seed seed-metering chamber device, which used the first- and second-level seed-picking scoops in a series arrangement, with a single-seed seeding rate of 95.38%; however, the problems included its complex structure, high mechanical costs, and difficult maintenance. Geng et al. [11] developed a pneumatic-controlled *garlic* single-seed seed-feeding spoon-chain device with a seeding rate of 93.50%, but the phenomenon of seed leakage was serious during operation, and it required manual reseeded. Li et al. [12] designed a *garlic* single-seed spoon-type seed-metering device with a laser sensor, taking the seed box as the core. This had excellent overall performance, but the equipment cost was high. Li et al. [13] developed a spoon-type *garlic* seed-metering device that used the cavity formed by the seed-harvesting spoon and the seed-metering wheel to conduct single-seed seeding, with a single-seed rate of 91.10%. However, *garlic* was not screened and graded before sowing, resulting in a high rate of missed sowing and reseeded. Li et al. [14] made a kind of automatic *garlic* seed box seed-metering device, which can accurately realize the single-seed placement of *garlic* seeds; however, the *garlic* seeds need to be manually placed in the seed box, which has a low degree of automation. Liang et al. [15] developed a seed-metering air suction device, but the suction plate could not adapt to the complex appearance of *garlic* seeds, resulting in a high missing rate.

Taking white *garlic* from Pizhou in the Jiangsu Province of China as the experimental material and drawing on the design concept of previous studies, this work studied a finger clip *garlic* disc seed-metering device. In this design, with the seed-metering device as the research object, a three-dimensional model was established, followed by the theory analysis of important component parameters; then, a discrete element simulation experiment and bench test were carried out to analyze the single factors’ implications for the filling effect. The optimal parameter combination was determined using the response surface method, which was compared with the bench test for validation purposes, providing significant data support for the optimization of *garlic* seed-metering device designs.

## 2. Materials and Methods

### 2.1. Structure and Working Principle of the Seed-Metering Device

#### Structure of the Seed-Metering Device

The finger clip *garlic* disc seed-metering device is composed of a seed discharger side plate, an intermediate partition, a falling seed guide, a seed-collecting spoon, a seed extraction splint-fixing box, a seeding tray, a seed press plate, a rotating shaft of seed pressers, a control execution board, a fine adjustment spring, a seed-opening and -closing control board, etc., as shown in Figure 1.

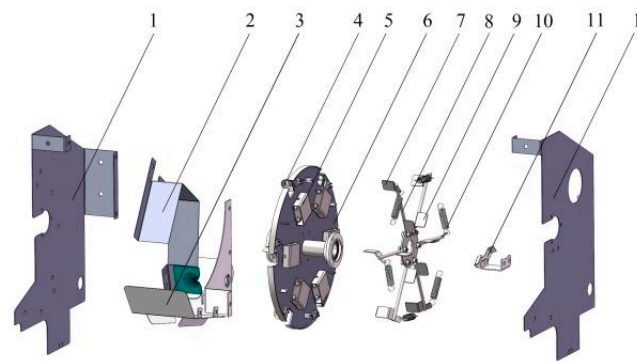


**Figure 1.** Schematic diagram of the seed-metering device: 1. the seed discharger side plate; 2. the intermediate partition; 3. the falling seed guide; 4. the seed-collecting spoon; 5. the seed extraction splint-fixing box; 6. the seeding tray; 7. the seed press plate; 8. the rotating shaft of seed pressers; 9. the control execution board; 10. the fine adjustment spring; 11. the seed-opening and -closing control board.

## 2.2. Working Principle of the Seed-Metering Device

This seed-metering device is designed with three working areas, namely a seed-filling area, a seed-carrying area, and a seed-dropping area, which are represented by I, II, and III, respectively [16], as shown in Figure 2. When the seed-metering device is in operation, the seed-opening and -closing control board is fixed and is jointly controlled with the fine adjustment spring. The clockwise rotation of the seeding tray drives the seed-collecting spoon to rotate into seed-dropping area III, and the control board contacts with the seed-opening and -closing control board. The closed seed press plate gradually overcomes the spring tension and synchronously rotates around the rotating axis of the seed-pressing plate, so that the seed-pressing plate is opened to the maximum space and rotates towards the seed-filling area I. In filling area I, *garlic* seeds are scooped into the seed-taking spoon and rotated towards seed-carrying area II. When entering seed-carrying area II, the control board is gradually separated from the seed-taking control board. Under the action of the resilience force of the fine adjustment spring, the seed-pressing plate is pulled close, and the *garlic* seeds are held before transportation through seed-carrying zone II to seed-dropping zone III. In seed-dropping area III, the control board contacts the seed-taking control board again, so that the closed seed press board is opened to the maximum space, and the *garlic* is planted using its own gravity and centrifugal force, and falls into the seed-dropping falling seed guide to complete the seeding process.

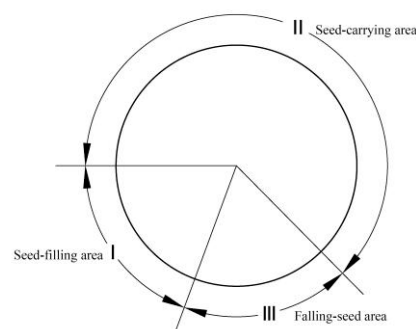


**Figure 2.** Zone I: seed-filling zone; Zone II: seed-carrying zone; Zone III: seed-dropping zone.

## 2.3. The Design of Critical Components

### Parameters of the Seed-Collecting Scoop

Seed-collecting scoop is the key component of the seed-metering device. To achieve an excellent performance, two factors should be taken into consideration in the size design: the size of *garlic* seed and *garlic* stance in the scoop. The *garlic* stance in the seed-taking

spoon can be divided into three states: the “lying posture”, the “side-lying posture”, and the “standing posture”, as shown in Figure 3.

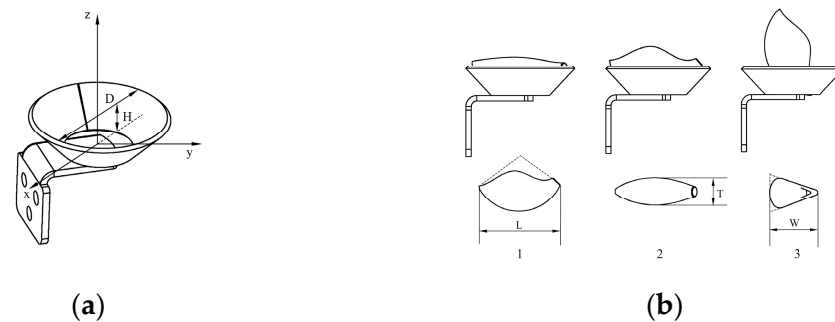


**Figure 3.** Seed-picking spoon size and *garlic* stance: (a) structure of the seed scoop; (b) *garlic* stance and vertical projection.

Oxyz is the coordinate system: 1 is the lying posture of *garlic* seeds; 2 is the side-lying posture of *garlic* seeds; 3 is the standing posture of *garlic* seeds; L is the length of *garlic* seeds in mm; T is the thickness of *garlic* seeds in mm; and W is the width of *garlic* seeds in mm.

Based on theoretical analysis [17], the distribution probability of *garlic* seeds in the scoop is positively correlated with the cross-sectional area of the “lying posture”, the “side-lying posture”, and the “standing posture”, and the probability sum is 1. Under normal circumstances, the projection of *garlic* in the three postures is approximately fan-shaped, elliptic, and triangular, respectively, and its area complies with the following equation:

$$\begin{cases} S_1 = \frac{\pi}{180} W_0^2 \arctan \frac{L_0}{W_0} \\ S_2 = \frac{\pi}{4} L_0 T_0 \\ S_3 = \frac{1}{2} W_0 T_0 \end{cases} \quad (1)$$

where  $S_1$  is the horizontal cross-sectional area of *garlic* seeds in the lying position,  $\text{mm}^2$ ;  $S_2$  is the horizontal cross-sectional area of *garlic* seeds in the lateral lying position,  $\text{mm}^2$ ;  $S_3$  is the horizontal cross-sectional area of *garlic* seeds in the standing position,  $\text{mm}^2$ ; the subscript 0 indicates the average value of each dimension.

In the *garlic* material experiment, 500 plump *garlic* seeds were randomly selected; their length L, width W, and thickness T were measured with a vernier caliper with a precision of 0.01 mm; and the average values were calculated, which were represented by  $L_0$ ,  $W_0$ , and  $T_0$ , respectively. All *garlic* seeds can be divided into three grades according to their size: grade 1 (small seeds), grade 2 (medium seeds), and grade 3 (large seeds). Table 1 showcases the statistical table of seed size at all levels.

**Table 1.** Three-dimensional sizes of seeds.

Size Levels	Average Length/mm	Average Width/mm	Average Thickness/mm
1	21.32	13.75	12.83
2	25.34	15.47	14.58
3	28.27	16.83	15.76

According to the three-dimensional sizes of *garlic* seeds in Table 1 and Formula (1), the maximum horizontal cross-sectional area was obtained in the state of “lying posture”. Combined with the principle of minimum potential energy, the size of the “lying posture” was taken as the basis of the design.

Regarding the length, in order to ensure that the scoop could accommodate 1 *garlic* seed in the state of the “lying posture”, and that the space is as large as possible to improve the seed rate, the opening diameter of the seed scoop D should be greater than or equal to the average length of *garlic* seed  $L_0$ . In order to prevent 2 “standing” *garlic* seeds from being filled into the seed taking spoon at the same time, the opening diameter of the seed-taking

spoon D should be less than or equal to the sum of the average width of 2 *garlic* seeds  $W_0$ . In the depth direction, in order to ensure that the seed scoop does not slip after seed collection, the depth H of the seed scoop should be greater than or equal to half of the average thickness  $T_0$  of *garlic* seeds, and less than or equal to half of the average length  $L_0$ . To ensure that more than 80% of seeds can be used, adjusting coefficients  $k_1$  and  $k_2$  were introduced, and the structural dimension parameters of seed scoop should meet Formula (2):

$$\begin{cases} L_0 \leq D \leq 2W_0 \\ D = k_1 L_0 \\ \frac{1}{2}T_0 \leq H \leq \frac{1}{2}L_0 \\ H = \frac{1}{2}k_2 T_0 \end{cases} \quad (2)$$

In the formula,  $k_1$  refers to the adjustment coefficient of the opening diameter of the seed scoop, which was set from 1 to 1.2.  $k_2$  is the depth adjustment coefficient of seed scoop, ranging from 1 to 1.3. The three-dimensional sizes of seeds in Table 1 were substituted into Formula (2), and three groups of parameter ranges for seed-picking spoons were obtained, as shown in Table 2. The depth range of the seed scoop shows little variation and exerts little influence on seed filling. The opening diameters of the three models were 21.32–25.58 mm, 25.34–30.41 mm, and 28.27–31.66 mm, so we chose the medians of 22, 26, and 30 mm for the initial determination of the parameters, and the same formula for the depth. Therefore, the value was set to 8 mm. The opening diameter of the seed scoop ranged from 22 mm to 30 mm.

**Table 2.** Seed extractor parameters.

Model	Diameter of the Opening/mm	Values Taken in This Article/mm	Depth/mm	Values Taken in This Article/mm
1	21.32~25.58	22	6.42~8.33	8
2	25.34~30.41	26	6.81~8.85	8
3	28.27~31.66	30	7.88~10.24	8

#### 2.4. Determine Parameters of the Seed-Filling Control Mechanism

The seed-filling control mechanism of the finger clip plate seed-metering device consisted of a seed-pressing plate, a control execution board, a rotating shaft of seed pressers, and a seed-opening and -closing control board. The control board was in contact with the open and close control board for seed taking. The movement of the seed-pressing board was driven by the torque of the rotating shaft seed presser to realize the seed-filling, seed-carrying, and seed-dropping potentials of *garlic* seeds, which has a direct impact on the working performance of the seed-metering device.

The working state of the seed-filling control mechanism is represented by the seed-filling duration angle, the finger-clamping closing angle, the finger clip seed-carrying angle, and the finger clip opening angle, as shown in Figure 4. In order to effectively improve seed-filling performance, the operation angle of the seed-filling area was designed to ensure stability. To ensure that the *garlic* seeds are held and carried smoothly, and to prevent the seed-pressing board from quickly closing and damaging the *garlic* seeds, the closed angle of the seed-taking control board was relatively flat. The control plate has a steep opening angle for seed picking, allowing the *garlic* seeds to be accurately brought into the seed drop area and the pressure plate to open quickly and accurately. According to the above design principles, and combined with the specific position of the population in the seed-filling area, the duration angle of seed filling was set as  $135^\circ$ , the finger clip closing angle was set as  $15^\circ$ , the finger clip carrying angle was set to  $200^\circ$ , and the finger clip opening angle was set as  $10^\circ$ , corresponding to the optimal working state of the seed-filling control mechanism, which ensured the ease and flexibility of seed filling, seed carrying, and seed dropping from the hardware design.

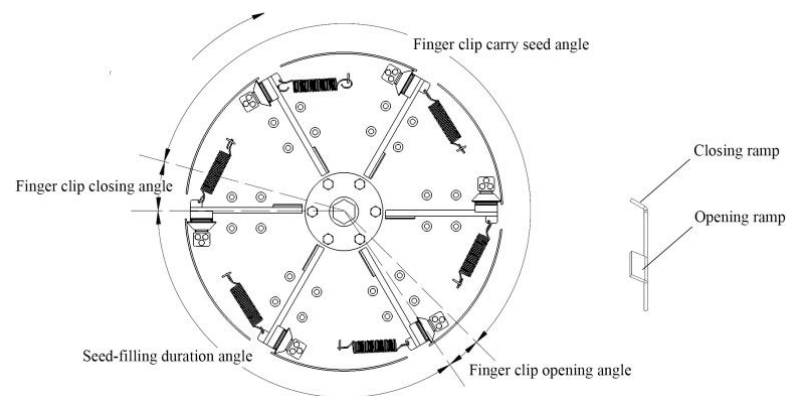


Figure 4. Seeding control mechanism movement phase.

According to Figure 4, when the angle of each working area is determined, the operating times of filling, carrying, and dropping were negatively correlated with the speed of the seed-metering device, thus affecting the working performance. Combined with the actual operating requirements of the seed-metering device, the initial value of speed is set as 15~45 r/min [18].

### 2.5. Determine the Garlic Parameters in the Seed-Filling Area

When the finger-clip-type garlic disc seed-metering device worked in the seed-filling area, the seed-taking scoop supported most of the weight of garlic seeds, and the seed-pressing plate maintained its relative stability. In the seed-filling area, a single garlic seed filled into the seed scoop was taken as the research object, and the garlic centroid was taken as the origin to establish a coordinate system: the x-axis direction was in the same direction as the inertial centrifugal force, while the y-axis direction was perpendicular to the inertial centrifugal force, as shown in Figure 5.

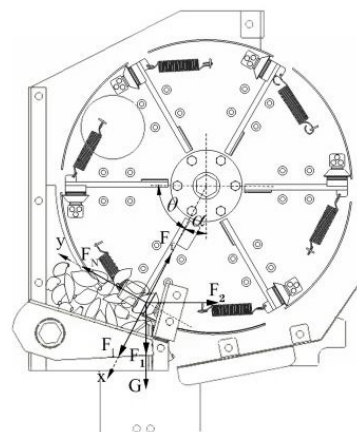


Figure 5. The diagram of force analysis of seeding process. Note: G is the gravity force of garlic species, (N);  $F_N$  is the support force of the seed-taking spoon to the garlic seed, N;  $F_f$  is the friction force between the garlic seed and the seed-taking scoop, N;  $F_1$  is the longitudinal combined pressure of the garlic seed, N;  $F_2$  is the horizontal combined pressure of the garlic seeds, N;  $\alpha$  is the angle between the x axis and the direction of gravity, ( $^\circ$ );  $\theta$  is the angle between  $F_1$  and  $F_2$ , ( $^\circ$ ).

The acting force on garlic seeds is shown in the equation below:

$$\begin{cases} F_1 < F_f + F_2 \cos \theta - (F_1 + G) \cos \alpha \\ F_N - (F_1 + G) \sin \alpha + F_2 \sin \theta = 0 \end{cases} \quad (3)$$

The inertia centrifugal force and friction between *garlic* seed and seed scoop correspond to the equations below:

$$\begin{cases} F_f = \mu F_N \\ G = mg \\ F_1 = \frac{mv^2}{R} \end{cases} \quad (4)$$

where  $\mu$  is the coefficient of friction between the *garlic* seed and the seed picker;  $m$  is the weight of the *garlic* seeds in kg;  $v$  is the operating speed.

$$v < \sqrt{\frac{\mu(F_1 \sin \alpha + G \sin \alpha - F_2 \sin \theta) + F_2 \cos \theta - (F_1 + G) \cos \alpha}{m}} \quad (5)$$

According to Equation (5), there is a certain connection between the operating speed of seeding discharger and the transverse and longitudinal pressure. The pressure is related to the population size and flow pattern, which has an influence on the filling effect of the seed-metering device. If the number of *garlic* seeds is too high, the lower *garlic* seeds will be over-compacted, which will lead to multiple *garlic* seeds entering the seed taking scoop and increasing the reply rate. If the number of *garlic* seeds is too low, the *garlic* seeds will be unable to be backfilled in time. The next level of seed-taking spoon will have inadequate seeds, so the missing rate will rise. Combined with the practical operation and theoretical analysis of the seed-metering device, the population range was preliminarily set as 120~360 seeds.

#### 2.6. EDEM Discrete Element Simulation

Through the above analyses, it was determined that the opening diameter of the scoop, the population number in the seed-filling area, and the operating speed were the main factors affecting the seed-filling performance of the seed-metering device. To further optimize the parameters, EDEM software was applied to analyze the discrete element single-factor simulation test, which provided a theoretical basis for the optimal design of the seed-metering device and its key components.

#### Simulation Model

The three-dimensional model of the seed-metering device was simplified and imported into the EDEM in.stl format. Based on the external dimensions of *garlic* species in Table 1, *garlic* seed particles were established through multi-sphere polymerization and filling [19]. We used 27 particles in this multi-sphere assembly, and the physical diameter of these spheres was between 1.49028 and 6.45019 mm, as shown in Figure 6a. The Hertz–Mindlin non-sliding contact model was selected as a contact model between particles and the seed-collecting device [20,21]. According to the application requirements of the seed-metering device, the material of each component of the seed-metering device was set as 45 steel. The basic simulation parameters are shown in Table 3. In order to meet the geometric size differences in *garlic* species within the actual population, the particle factory and random distribution functions were exerted to randomly generate *garlic* species, and the distribution coefficient was 0.92~1.07 times the size of the *garlic* species model. The add linear rotation instruction in the add kinematic module was mainly applied to the seed row circling and the opening and closing of the seed-taking scoop. The fixed time-step was set to 20% of the Rayleigh time-step, and the mesh size was determined to be twice that of the minimum radius. The working state of the seed-metering device in the simulation process is shown in Figure 6b.



**Figure 6.** Simulation model and simulation working state diagram. (a) Multi-sphere representation of the *garlic* seeds; (b) EDEM simulation of the seed rower operating state.

**Table 3.** Simulation parameters of *garlic* seed picking.

Parameters	45 Steel	Garlics
Density/( $\text{kg}\cdot\text{m}^{-3}$ )	7800	1080
Poisson ratio	0.250	0.230
Young's modulus/Pa	$2.5 \times 10^9$	
Coefficient of restitution	0.432	0.483
Static friction factor	0.466	0.502
Dynamic friction factor	0.214	0.108

### 2.7. Test Materials and Equipment

The test materials are shown in Figure 7a. The test was carried out in the Agricultural Machinery Laboratory of Nanjing Agricultural University in China with self-made bench test equipment. The seed-metering device was fixed on the mounting rack and connected to the AC gear speed regulating motor (the speed was continuously adjustable from 0 to 54 r/min). The operating speed of the seed-metering device was controlled by the AC governor, as shown in Figure 7b, alongside a certain quantity of seeds. The test method refers to GB/T6973-2005 "Single Seed (Precision) Discharge Test Method". Since the sum of the missing rate, replay rate, and qualified rate is 100%, the core purpose of the seed-metering device design is to improve the qualified rate of single *garlic* seeds and reduce the missing rate. Therefore, the missing rate  $Y_1$  and qualified rate  $Y_2$  were selected as evaluation indicators. After the seed-metering device was stable, the seed-metering device was counted 200 times, and each group was repeated 3 times. The average value of the results was taken to obtain the missing rate and qualified rate data.

### 2.8. Experimental Factors and Evaluation Indicators

Based on pre-experiments, the opening diameter of seed scoop  $X_1$ , the number of seeds in the chamber population  $X_2$ , and the operating speed  $X_3$  were selected as test factors, and the missing rate  $Y_1$  and qualified rate  $Y_2$  were selected as response indicators. According to the preliminary theoretical analysis and pre-experiment, the value range of each factor was determined: the opening diameter  $R$  of the scoop was 24~28 mm, the population was 160~320 seeds, and the operating speed of the seed-metering apparatus was 25~35 r/min. Under the Box–Behnken experimental design method, three-factor and three-level orthogonal tests were conducted [22]. The test factors and levels are shown in Table 4.





**Figure 7.** Test materials and bench. (a) *Garlic* of Pizhou; (b) 1. motor governor; 2. seed-filling chamber; 3. mounting rack; 4. seeding tray; 5. seed-taking device.

**Table 4.** Factors and levels of test.

Levels	Diameter of the Opening $X_1/\text{mm}$	Number of Seeds $X_2$	Operating Speed $X_3/(\text{m}\cdot\text{s}^{-1})$
−1	24	160	25
0	26	240	30
1	28	320	35

According to the National Standard of P.R.C (GB/T 6973-2005 Testing Methods of Single-Seed Drills (Precision Drills)) [23], the qualified rate of single-seed  $Q$ , the reply rate  $M$ , and the missing rate  $C$  were taken as evaluation indicators [24], and the specific formula is shown in Equation (6).

$$\begin{cases} Q = \frac{N_1}{N} \times 100\% \\ M = \frac{N_2}{N} \times 100\% \\ C = \frac{N_3}{N} \times 100\% \end{cases} \quad (6)$$

where  $N$  is the theoretical number of seeds sown;  $N_1$  is the number of single seeds;  $N_2$  is the reseeding number;  $N_3$  is the number of missed seeds.

### 3. Results and Discussion

#### 3.1. Single-Factor Simulation Analysis

##### 3.1.1. Influence of Population Size on Seed-Filling Performance

According to the practical experience of *garlic* sowing, the opening diameter of the seed scoop was set as 26 mm, and the operating speed was set as 30 r/min. A particle factory was set in the EDEM pre-processing module to generate seven levels of 120, 160, 200, 240, 280, 320, and 360 seeds, respectively, and the simulation experiment was conducted. The effects of different population numbers on seed-filling performance were analyzed to determine the population range of high-quality seed filling. The dynamic particle plant generates falling *garlic* seeds at a rate of 3 pcs/s to maintain the population number, as shown in Figure 8. As demonstrated by the diagram, with an increase in the *garlic* population in the seed-filling room, the missing rate gradually decreased, the reply rate gradually increased, and the qualified rate of a single seed showed a tendency to first increase and then decrease.

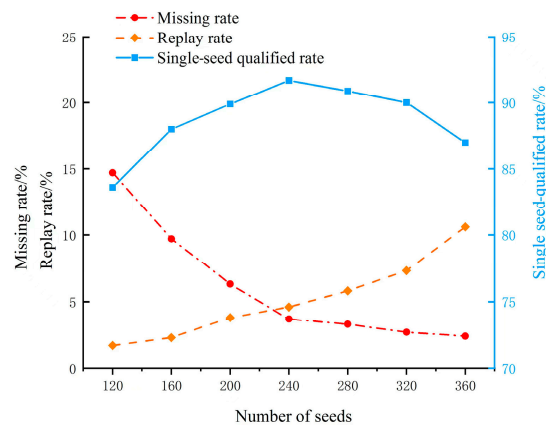


**Figure 8.** Relationship with evaluation indicators under different population numbers.

When the population in the seed-filling area was below 160 seeds, only a few *garlic* populations flowed to the edge of the area for backfilling due to the low *garlic* population (as shown in Figure 9), and the next seed-taking scoop entered the seed-filling area. This could not guarantee enough stable *garlic* species in the seed-filling area, leading to an increase in the missing rate. When the population number in the seed-filling area was more than 320 seeds, there were enough stable *garlic* seeds in the seed-filling area for seed-filling (as shown in Figure 10), and the missed sowing rate decreased. When “floating” out of the seed layer, they often carried extra *garlic* seeds, increasing the replay rate.

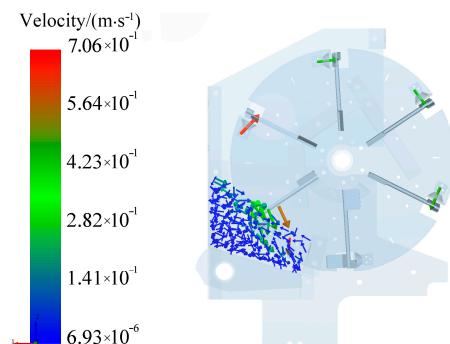


**Figure 9.** *Garlic* seed movement when the population was below 160 grains.

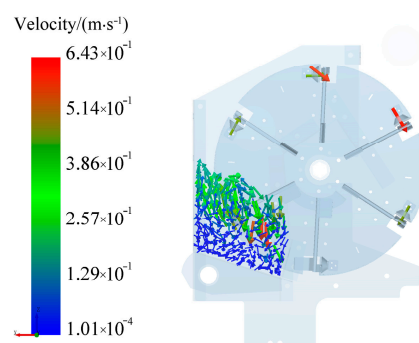


**Figure 10.** *Garlic* seed movement when the population was above 320 grains.

The results show that the number of the high-quality population ranged from 160 to 320. When the population number was 240, the qualified rate of a single seed was more than 90%, and seed filling reached optimal performance.

### 3.1.2. Influence of Seed-Taking Scoop Opening Diameter on Seed-Filling Performance

According to the analysis results, 240 *garlic* seeds were selected; the operating speed was set at 30 r/min; and the opening diameters of the seed scoop were set at 22 mm, 24 mm, 26 mm, 28 mm, and 30 mm. Simulation tests were conducted to analyze the influence of seed scoop opening diameters on seed-filling performance, and then determine the diameter range of its high-quality seed-filling; the results are shown in Figure 11. With the rise in the opening diameter of the seed scoop, the missing rate decreased and the reply rate increased, and the qualified rate of single seeds first increased and then decreased.

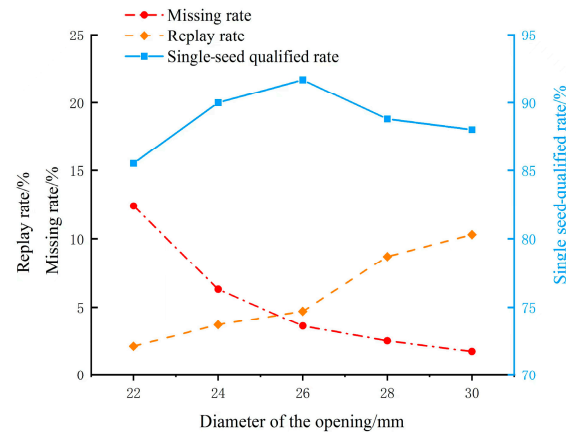


**Figure 11.** Relationship with evaluation indicators under different opening radii.

When the opening diameter of the seed-taking scoop was less than 24 mm, it could not accommodate the larger *garlic* species. When it “surfaced” the seed layer, the *garlic* species were taken out of the population by the seed scoop in the “standing” state (as shown in Figure 12). The unstable stress state made the *garlic* population prone to falling in the process, resulting in an increase in the missing rate. When the opening diameter of the seed-taking scoop was larger than 28 mm, it could accommodate several small *garlic* seeds. When the seed-taking scoop “surfaced” the seed layer, *garlic* seeds in the middle scoop had both a “lying posture” and other relatively stable states (as shown in Figure 13), resulting in an increase in the reply rate.

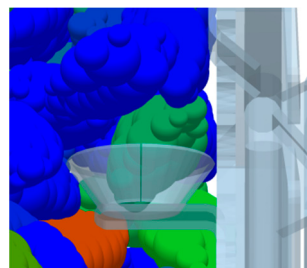


**Figure 12.** Vertical unstable state.



**Figure 13.** Replay status.

From this experiment, it can be concluded that the opening diameter of the seed-taking scoop ranged from 24 mm to 28 mm, and when the opening diameter was 26 mm, the qualified rate of the single seed was more than 90%, and the seed-filling performance was the best.

### 3.1.3. Influence of Operating Speed on Seed-Filling Performance

In the analysis results, 240 *garlic* seeds were selected; the diameter of the seed scoop was set as 26 mm; and the operating speed was set as 15 r/min, 20 r/min, 25 r/min, 30 r/min, 35 r/min, 40 r/min, and 45 r/min. A simulation test was conducted to analyze the influence of the operating speed of the seed tray on seed-filling performance and determine the speed range of its high-quality seed-filling, as shown in Figure 14. As can be seen from the diagram, with the rise in operating speed, the missing rate gradually increased, the replay rate gradually decreased, and the qualified rate of single seed showed a trend of first increasing and then decreasing. When the operating speed was less than 25 r/min, the filling time of single-seed scoops was longer, and the *garlic* seed was fully backfilled, which made it easy to pick more than one seed per scoop. The replay rate increased, and the missing rate decreased. When the operating speed was greater than 35 r/min, the number of high-speed *garlic* seeds obviously increased, the population backfilling was not sufficient, and the *garlic* seeds were hard to scoop; as a result, the replay rate decreased and the missing rate increased.

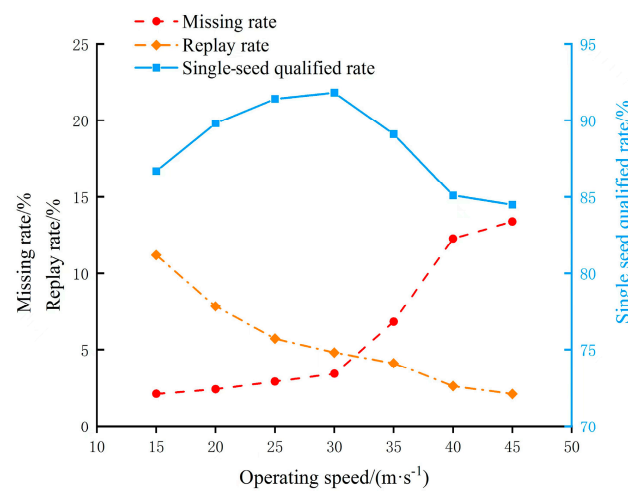


Figure 14. Relationship with evaluation indicators under different operating speeds.

From this test, the quality range of operating speeds was 25~35 r/min. When the operating speed was 30 r/min, the single-seed qualified rate was more than 90%, and the seed-filling performance achieved the best effect.

### 3.2. Box–Behnken Design Experiment

#### Experimental Design and Results

The experiment design scheme and results are shown in Table 5. The Design Expert 13 data analysis software was applied to conduct a multiple regression fitting analysis on the experimental data [25,26], and the regression equation of the missing rate  $y_1$  and the single-seed qualified rate  $y_2$  was obtained as below.

$$\begin{cases} y_1 = 3.24 - 1.72x_1 - 1.44x_2 + 1.11x_3 + 0.225x_1x_2 + 0.025x_1x_3 \\ \quad - 0.35x_2x_3 + 1.13x_1^2 + 1.31x_2^2 - 0.295x_3^2 \\ y_2 = 92.40 - 0.375x_1 - 0.55x_2 - 0.35x_3 - 0.525x_1x_2 + 0.175x_1x_3 \\ \quad - 0.075x_2x_3 - 2.04x_1^2 - 1.19x_2^2 - 0.8875x_3^2 \end{cases} \quad (7)$$

**Table 5.** Experiment design and results.

No.	Diameter of the Opening $X_1/\text{mm}$	Number of Seeds $X_2$	Operating Speed $X_3/(\text{m}\cdot\text{s}^{-1})$	Missing Rate $y_1/\%$	Single-Seed Qualified Rate $y_2/\%$
1	-1	-1	0	9.2	89.6
2	1	-1	0	5.1	89.8
3	-1	1	0	5.8	89.6
4	1	1	0	2.6	87.7
5	-1	0	-1	4.6	90.3
6	1	0	-1	1.3	89.3
7	-1	0	1	6.8	89.3
8	1	0	1	3.6	89.0
9	0	-1	-1	4.2	91.2
10	0	1	-1	2.1	90.2
11	0	-1	1	7.1	90.6
12	0	1	1	3.6	89.3
13	0	0	0	3.4	92.0
14	0	0	0	3.1	92.6
15	0	0	0	3.4	92.4
16	0	0	0	3.3	92.4
17	0	0	0	3.0	92.6

The test results and variance analysis results of the regression equation are shown in Table 6. It can be concluded that the fitting degree of the leakage charge rate and the single-seed qualified rate in the regression model was extremely significant ( $p < 0.01$ ), and the missing items of each regression model were not significant ( $p > 0.05$ ), indicating that the fitting degree of the regression model was high. The determination coefficients were 0.9739 and 0.9759, respectively, indicating that the regression model complied with more than 97% of the sample data. According to a variance analysis, the order of influence of test factors on missing rate was  $X_1 > X_2 > X_3$  and the order of influence on the single-seed qualified rate was  $X_2 > X_1 > X_3$ .

3.3. Response Surface Analysis

According to the regression model of the single-seed qualified rate and missing rate, one of the test factors was set at 0, and the effects of other factors on the test indicator were further discussed. The response diagram was drawn by using Design-Expert 13, as shown in Figure 15.

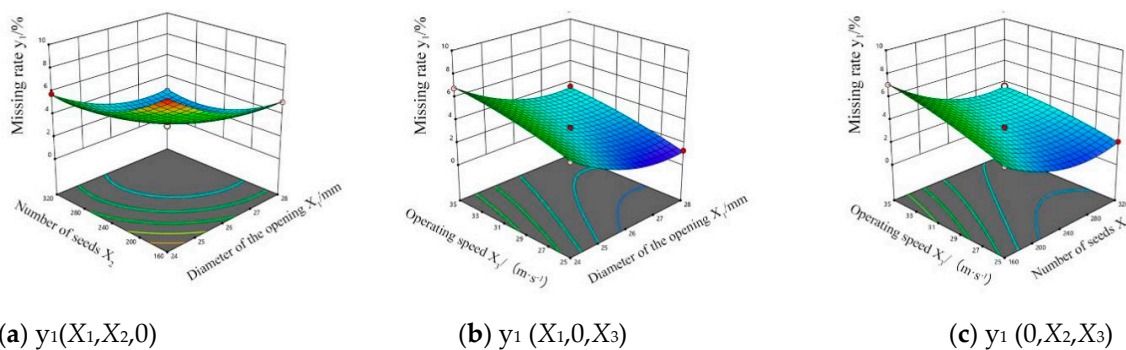


**Figure 15.** Effect of test factors on the missing rate.

**Table 6.** Variance analysis of regression model.

Size Levels	Source	Sum of Square	df	Mean Square	F Value	p Value
Missing rate $y_1$	Model	64.28	9	7.14	222.69	<0.0001 **
	$X_1$	23.80	1	23.80	742.25	<0.0001 **
	$X_2$	16.53	1	16.53	515.45	<0.0001 **
	$X_3$	9.90	1	9.90	308.72	<0.0001 **
	$X_1X_2$	0.2025	1	0.2025	6.31	0.0402 *
	$X_1X_3$	0.0025	1	0.0025	0.0780	0.7882
	$X_2X_3$	0.4900	1	0.4900	15.28	0.0058 **
	$X_1^2$	5.38	1	5.38	167.64	<0.0001 **
	$X_2^2$	7.17	1	7.17	223.58	<0.0001 **
	$X_3^2$	0.3664	1	0.3664	11.43	0.0118 *
	Residual	0.2245	7	0.0321		
	Lack of fit	0.0925	3	0.0308	0.9343	0.5023
	Pure error	0.1320	4	0.0330		
Cor total	64.50	16				
Single-seed qualified rate $y_2$	Model	35.15	9	3.91	101.25	<0.0001 **
	$X_1$	1.12	1	1.12	29.17	0.0010 **
	$X_2$	2.42	1	2.42	62.74	<0.0001 **
	$X_3$	0.9800	1	0.9800	25.41	0.0015 **
	$X_1X_2$	1.10	1	1.10	28.58	0.0011 **
	$X_1X_3$	0.1225	1	0.1225	3.18	0.1179
	$X_2X_3$	0.0225	1	0.0225	0.5833	0.4700
	$X_1^2$	17.48	1	17.48	453.17	<0.0001 **
	$X_2^2$	5.94	1	5.94	153.94	<0.0001 **
	$X_3^2$	3.32	1	3.32	85.98	<0.0001 **
	Residual	0.2700	7	0.0386		
	Lack of fit	0.0300	3	0.0100	0.1667	0.9136
	Pure error	0.2400	4	0.0600		
Cor total	35.42	16				

Note: \* represents significant difference ( $p < 0.05$ ); \*\* represents extremely significant difference ( $p < 0.01$ ).

### (1) Influence of various test factors on missing rate

As shown in Figure 15a, when the operating speed was at level 0 (30 r/min) and the opening diameter of the seed scoop was kept constant, the missing rate decreased with an increase in the population in the seed-filling area. When the population in the filling area was constant, the missing rate decreased with an increase in the opening diameter of the scoop. Figure 15b shows that the population was at level 0 (240 seeds). When the opening diameter of the seed scoop was the same, the missing rate rose with an increase in the operating speed. When the operating speed was constant, the missing rate decreased with a larger opening diameter. According to Figure 15c, the opening diameter was set to level 0 (26 mm). When the population number was constant, the missing rate ascended with a rise in the operating speed. When the operating speed was the same, the missing rate descended with an increase in the opening diameter.

### (2) The influence of various experimental factors on the qualified rate

Figure 16a indicates that when the operating speed was at level 0 (30 r/min) and the opening diameter of seed scoop was constant, the qualified rate of single seeds first increased and then decreased with an increase in the population. When the population was constant, the single-seed qualified rate first increased and then decreased with a rise in the scoop opening diameter. It can be seen from Figure 16b that, when the population was at level 0 (240 grains) and the opening diameter of the seed-taking scoop remained the same, the single-seed qualified rate first increased and then decreased with an increase in the operating speed. When the operating speed was constant, the qualified rate of the single seed first increased and then decreased with an increase in the opening diameter. Figure 16c shows that when the opening diameter of the seed scoop was at level 0 (26 mm) and the

population number was constant, the qualified rate of single seeds first increased and then decreased with a larger operating speed. When the operating speed was constant, the single-seed qualified rate first increased and then decreased with an increase in the population.

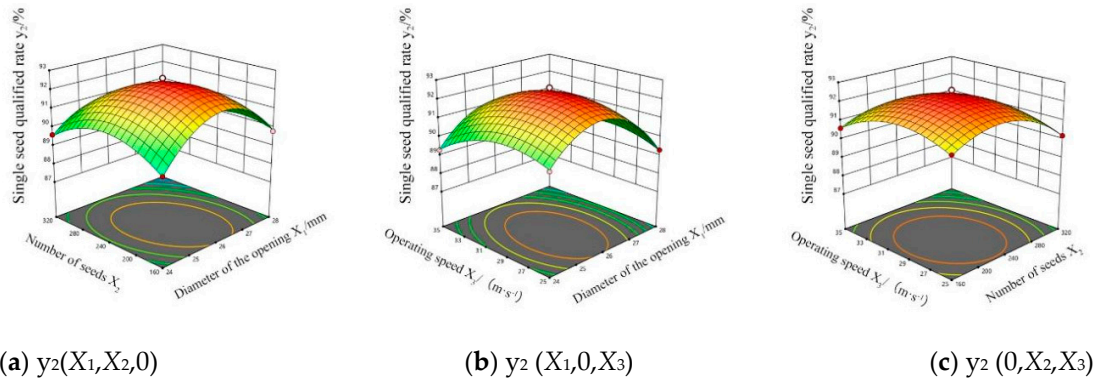


Figure 16. Effect of test factors on qualified rate.

### 3.4. Parameter Optimization and Experiment Verification

To achieve the optimal performance of the test bench, the influencing factors in the test were optimized. The objective function and constraint conditions were as follows:

$$\begin{cases} \min y_1 \\ \max y_2 \\ \text{s.t.} \begin{cases} 22 \leq X_1 \leq 28 \\ 160 \leq X_2 \leq 320 \\ 25 \leq X_3 \leq 35 \end{cases} \end{cases} \quad (8)$$

Optimization numerical strategies were applied to find the optimal parameter combination; the results obtained were as follows. The opening diameter of the seed-taking scoop was 26.14 mm, the population was 261.5 grains, and the operating speed was 27.95 r/min. The model predicted that the single-seed qualified rate, missing rate, and replay rate were 92.12%, 2.37%, and 5.52%, respectively. After rounding, the opening diameter of the seed-taking scoop was set at 26 mm and the operating speed was set at 28 r/min. The test method was carried out with 260 seeds at the center and 20 *garlic* seeds as a level, and the population number ranged from 200 to 320 seeds. When the seed layer number was 240~280, the operation effect reached the optimal effect, and the average single-seed qualified rate, missing rate, and replay rate were 91.86%, 2.71%, and 5.43%, respectively, as seen in Figure 17.

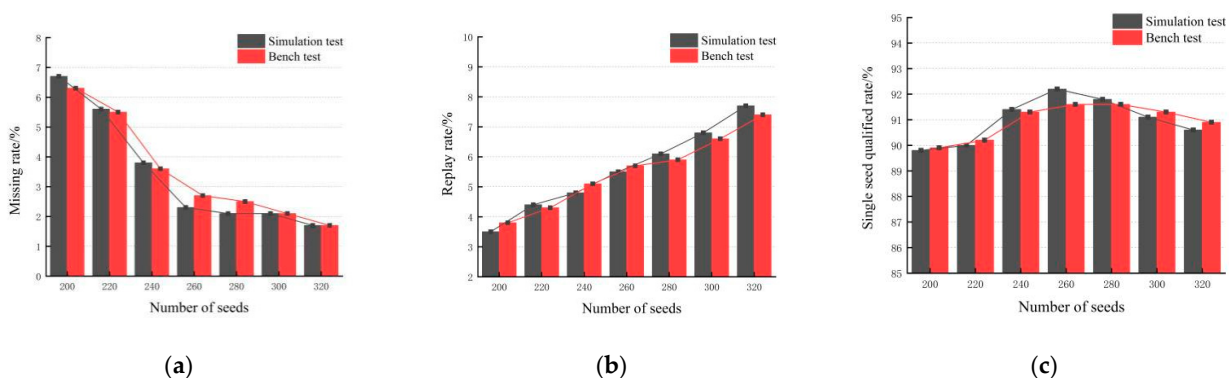


Figure 17. Simulation and experiment variation tendency of seeding process. (a) Missing rate; (b) replay rate; (c) single-seed qualified rate.

#### 4. Conclusions

The finger clip disc *garlic* seed-metering device adopts the fine adjustment spring and seed-opening and -closing control board to achieve seed taking and seed dropping. Using a theoretical design, the range of key structural parameters was determined, and the key parameters affecting the performance of the seed-metering device were found.

A single factor simulation test was carried out by discrete element simulation software EDEM. The effects of the population number, seed-taking scoop-opening diameter, and operating speed on seed-filling performance were analyzed; the specific reasons explaining the replies and missing seed were clarified; and the reasonable range of each parameter was preliminarily determined. The dosing coefficients of *garlic* seeds depended on the population ranges, the opening diameter, and the operating speed. Therefore, it is necessary to conduct single-factor tests. The single-factor simulation analysis shows that seeding performance was better when high-quality population ranged from 160 to 320, the opening diameter of the seed-taking scoop ranged from 24 mm to 28 mm, and the quality range of the operating speed was 25~35 r/min.

The Box–Behnken center combination method was used to carry out three-factor and three-level regression orthogonal tests. Response surface regression models were established as evaluation indicators for the missing rate and single-seed qualified rate, respectively, and the effects of the opening diameter, operating speed, and population number on evaluation indicators were obtained. The combination of optimized parameters after rounding was as follows: the opening diameter of the scoop was 26 mm, the operating speed was 28 r/min, and the population range was 240~280. Under the optimal combination of parameters, the bench test was carried out. As a result, the missing rate reached 2.71%, and the qualified rate of single seeds was 91.86%. The indicators are basically consistent with the experimental prediction, which demonstrates the reliability of the optimized model.

**Author Contributions:** Conceptualization, H.W., X.S., H.L. (Hua Li), X.Z. and Y.W.; methodology, H.W. and X.S.; software, H.W. and X.S.; validation, H.W.; formal analysis, H.W. and X.S.; investigation, H.W.; resources, H.W.; data curation, H.W. and X.S.; writing—original draft preparation, H.W.; writing—review and editing, H.W., X.S., H.L. (Hua Li), J.F., X.Z., Y.X., Y.W., H.L. (Huaqing Liu) and Z.L.; supervision, H.L. (Hua Li); funding acquisition, H.L. (Hua Li). All authors have read and agreed to the published version of the manuscript.

**Funding:** This research was supported by Jiangsu Modern Agricultural Industry Key Technology Innovation Project (CX(19)2007), Innovation Training Project for Jiangsu University students (202110307134Y), and sub-project 4 of Jiangsu middle and late mature *garlic* industrial cluster construction: *Garlic* mechanical intelligent operation technology and demonstration and promotion of green production technology.

**Data Availability Statement:** The data provided in this study are available upon request from the corresponding author. For privacy reasons, these data cannot be made public.

**Acknowledgments:** We acknowledge the financial support of the Jiangsu middle late *garlic* industry cluster sub project “demonstration and promotion for the technology of mechanization intelligent operation and green production for the *garlic*”.

**Conflicts of Interest:** The authors declare no conflict of interest.

#### References

1. Botas, J.; Fernandes, A.; Barros, L.; Alves, M.J.; Carvalho, A.M.; Ferreira, I. A Comparative Study of Black and White *Allium sativum* L.: Nutritional Composition and Bioactive Properties. *Molecules* **2019**, *24*, 2194. [[CrossRef](#)] [[PubMed](#)]
2. Gabriel, T.; Vestine, A.; Kim, K.D.; Kwon, S.J.; Sivanesan, I.; Chun, S.C. Antibacterial Activity of Nanoparticles of Garlic (*Allium sativum*) Extract against Different Bacteria Such as *Streptococcus mutans* and *Poryphomonas gingivalis*. *Appl. Sci.* **2022**, *12*, 3491. [[CrossRef](#)]
3. Zhou, X.J.; Dou, Y.X.; Huang, X.X.; Li, G.; Zhang, H.R.; Jiang, D.G.; Fan, J.P.; Condori-Apfata, J.A.; Liu, X.Q.; Condori-Pacsi, S.J.; et al. Using Principal Component Analysis and RNA-Seq to Identify Candidate Genes That Control Salt Tolerance in Garlic (*Allium sativum* L.). *Agronomy* **2021**, *11*, 691. [[CrossRef](#)]



4. Li, Y.H.; Wu, Y.Q.; Li, T.H.; Niu, Z.R.; Hou, J.L. Design and experiment of adjustment device based on machine vision for garlic clove direction. *Comput. Electron. Agric.* **2020**, *174*, 105513. [[CrossRef](#)]
5. Guo, H.P.; Cao, Y.Z.; Song, W.Y.; Zhang, J.; Wang, C.L.; Wang, C.S.; Yang, F.Z.; Zhu, L. Design and Simulation of a Garlic Seed Metering Mechanism. *Agriculture* **2021**, *11*, 1239. [[CrossRef](#)]
6. Shi, S.; Zhang, D.X.; Yang, L.; Cui, T.; Li, K.H.; Yin, X.W. Simulation and verification of seed-filling performance of pneumatic-combined holes maize precision seed-metering device based on EDEM. *Trans. Chin. Soc. Agric. Eng.* **2015**, *31*, 62–69. [[CrossRef](#)]
7. Geng, A.J.; Zhang, Z.L.; Song, Z.H.; Yang, J.N.; Li, R.X.; Hou, J.L.; Liu, S.Q. Kinematic analysis and parameter optimized experiment of garlic box putting process. *Trans. Chin. Soc. Agric. Eng.* **2016**, *32*, 29–35. [[CrossRef](#)]
8. Wu, W.J.; Tang, H.; Wang, Q.; Zhou, W.Q.; Yang, W.P.; Shen, H.G. Numerical simulation and experiment on seeding performance of pickup finger precision seed-metering device based on EDEM. *Trans. Chin. Soc. Agric. Eng.* **2015**, *31*, 43–50. [[CrossRef](#)]
9. Hou, J.L.; Wang, H.X.; Niu, Z.R.; Xi, R.; Li, T.H. Discrete element simulation and experiment of picking and clearing performance of garlic seed-picking device. *Trans. Chin. Soc. Agric. Eng.* **2019**, *35*, 48–57. [[CrossRef](#)]
10. Hou, J.L.; Liu, Q.C.; Li, T.H.; Li, Y.H.; Lou, W.; Geng, A.J. Design and experiment of the garlic seed metering device with double seed-filling chambers. *Trans. Chin. Soc. Agric. Eng.* **2021**, *37*, 21–32. [[CrossRef](#)]
11. Geng, A.J.; Li, X.Y.; Hou, J.L.; Zhang, Z.L.; Zhang, J.; Chong, J. Design and experiment of automatic directing garlic planter. *Trans. Chin. Soc. Agric. Eng.* **2018**, *34*, 17–25. [[CrossRef](#)]
12. Li, T.H.; Zhang, H.K.; Han, X.L.; Li, Y.H.; Hou, J.L.; Shi, G.Y. Design and experiment of missing seed detection and the reseeding device for spoon chain garlic seeders. *Trans. Chin. Soc. Agric. Eng.* **2022**, *38*, 24–32. [[CrossRef](#)]
13. Li, Y.H.; Zhang, Z.L.; Li, T.H.; Wu, Y.Q.; Niu, Z.R.; Hou, J.L. Design and Experiment of Wheel-spoon Type Garlic Precision Seed-picking Device. *Trans. Chin. Soc. Agric. Mach.* **2020**, *51*, 61–68.
14. Li, X.Y.; Geng, A.J.; Hou, J.L.; Ji, Z.; Zhang, Z.L. Design and experiment of full-automatic lifting and releasing device of garlic seed box. *Trans. Chin. Soc. Agric. Eng.* **2017**, *33*, 32–37. [[CrossRef](#)]
15. Xie, D.B.; Zhang, C.L.; Wu, X.Q.; Wang, W.W.; Liu, L.C.; Chrn, L.Q. Design and Test of Garlic Seed Placer with Seed Disturbing Tooth Assisted Air Suction. *Trans. Chin. Soc. Agric. Mach.* **2022**, *53*, 47–57. [[CrossRef](#)]
16. Han, D.D.; Zhang, D.X.; Jing, H.R.; Yang, L.; Cui, T.; Ding, Y.Q.; Wang, Z.D.; Wang, Y.X.; Zhang, T.L. DEM-CFD coupling simulation and optimization of an inside-filling air-blowing maize precision seed-metering device. *Comput. Electron. Agric.* **2018**, *150*, 426–438. [[CrossRef](#)]
17. Gao, X.J.; Cui, T.; Zhou, Z.Y.; Yu, Y.B.; Xu, Y.; Zhang, D.X.; Song, W. DEM study of particle motion in novel high-speed seed metering device. *Adv. Powder. Technol.* **2021**, *32*, 1438–1449. [[CrossRef](#)]
18. Wang, Y.B.; Li, H.W.; Hu, H.N.; He, J.; Wang, Q.J.; Lu, C.Y.; Liu, P.; He, D.; Lin, X. DEM-CFD coupling simulation and optimization of a self-suction wheat shooting device. *Powder Technol.* **2021**, *393*, 494–509. [[CrossRef](#)]
19. Sun, K.; Yu, J.Q.; Liang, L.S.; Wang, Y.; Yan, D.X.; Zhou, L.; Yu, Y. A DEM-based general modelling method and experimental verification for wheat seeds. *Powder Technol.* **2022**, *401*, 117353. [[CrossRef](#)]
20. Dun, G.Q.; Mao, N.; Gao, Z.Y.; Wu, X.P.; Liu, W.H.; Zhou, C. Model construction of soybean average diameter and hole parameters of seed-metering wheel based on DEM. *Int. J. Agric. Biol. Eng.* **2021**, *14*, 101–110. [[CrossRef](#)]
21. Xu, J.; Wang, X.M.; Zhang, Z.B.; Wu, W.B. Discrete Element Modeling and Simulation of Soybean Seed Using Multi-Spheres and Super-Ellipsoids. *IEEE Access* **2020**, *8*, 222672–222683. [[CrossRef](#)]
22. Sun, X.P.; Li, H.; Qi, X.D.; Nyambura, S.M.; Yin, J.Q.; Ma, Y.L.; Wang, J.S. Performance Parameters Optimization of a Three-Row Pneumatic Precision Metering Device for Brassica chinensis. *Agronomy* **2022**, *12*, 1011. [[CrossRef](#)]
23. Li, Z.D.; Yang, W.C.; Wu, Y.Y.; He, S.; Wang, W.W.; Chen, L.Q. Performance analysis and experiments of seed filling assisted by groove-tooth of pneumatic disc precision metering device for rapeseed. *Trans. Chin. Soc. Agric. Eng.* **2020**, *36*, 57–66. [[CrossRef](#)]
24. Lü, J.; Yang, Y.; Li, Z.; Shang, Q.Q.; Li, J.C.; Liu, Z.Y. Design and experiment of an air-suction potato seed metering device. *Int. J. Agric. Biol. Eng.* **2016**, *9*, 33–42. [[CrossRef](#)]
25. Sugirbay, A.M.; Zhao, J.; Nukeshev, S.O.; Chen, J. Determination of pin-roller parameters and evaluation of the uniformity of granular fertilizer application metering devices in precision farming. *Comput. Electron. Agric.* **2020**, *179*, 105835. [[CrossRef](#)]
26. Wang, J.W.; Qi, X.; Xu, C.S.; Wang, Z.M.; Jiang, Y.M.; Tang, H. Design Evaluation and Performance Analysis of the Inside-Filling Air-Assisted High-Speed Precision Maize Seed-Metering Device. *Sustainability* **2021**, *13*, 5483. [[CrossRef](#)]